

Supplementary information for

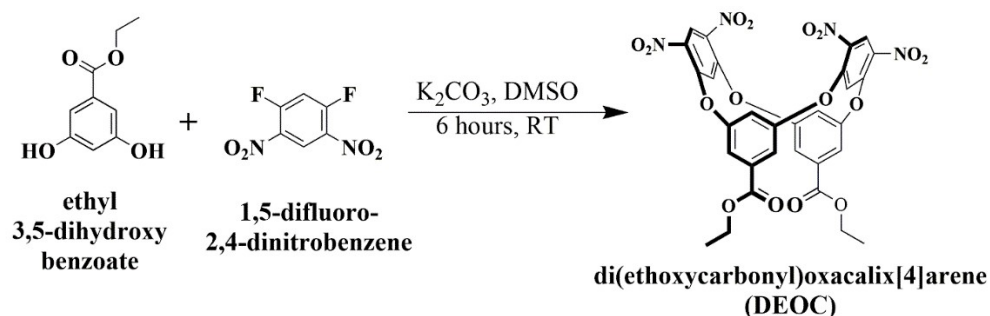
## Oxacalix[4]arene derived dual-sensing fluorescent probe for relay recognition of $\text{Hg}^{2+}$ and $\text{S}^{2-}$ ions

Manoj Vora, Shuvankar Dey, Anita Kongor, Manthan Panchal, Falak Panjwani, Ashukumar Verma, Vinod Jain\*

Department of Chemistry, School of Sciences, Gujarat University, Ahmedabad – 380009, Gujarat, India

### S1. Synthesis of di(ethoxy carbonyl)oxacalix[4]arene (DEOC)

The parent oxacalix[4]arene platform (DEOC) has been synthesized by following the previously reported method by our group. Typically, to the mixture of ethyl-3,5-dihydroxybenzoate (1.0g, 5.49mmol) and  $\text{K}_2\text{CO}_3$  (1.90g, 13.73mmol) in DMSO, 1,5-difluoro-2,4-dinitrobenzene (1.12g, 5.49mmol) was added, and the mixture was then stirred for 6 hours at room temperature. The progress of the reaction was monitored through TLC. After completion of the reaction, the organic layer was extracted with ethyl acetate, dried over  $\text{Na}_2\text{SO}_4$  and evaporated under reduced pressure to obtain yellow powder of di(ethoxycarbonyl)oxacalix[4]arene (DEOC) with 86% yield. Further, the crude was purified through column chromatography using a silica-gel with ethyl acetate/hexane (2/8) as eluent.



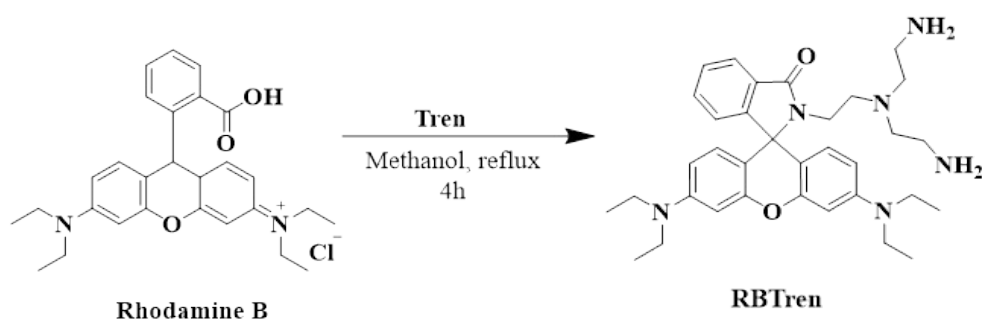
Scheme S1 Synthetic route for parent oxacalix[4]arene platform (DEOC)

### S2. Synthesis of RBTren

To a 30 ml solution of rhodamine B (1.00 g, 2.24 mmol) in methanol, tris(2-aminoethyl)-amine (5.92 ml, 4.50 mmol) was added and the reaction mixture was allowed to reflux for 4h until the fluorescence of rhodamine B disappeared. The progress of the reaction was monitored with TLC. After completion of the reaction, the solvent was evaporated in *vacuo* under reduced pressure. A small amount of water was added to the crude product and extracted with dichloromethane (100

ml) three times. The organic phase was separated, washed three times with brine solution and dried over  $\text{Na}_2\text{SO}_4$ . After filtration of  $\text{Na}_2\text{SO}_4$ , the solvent was removed under reduced pressure to give a product, RbTren as light orange oil in 82% yield.

ESI-MS: calcd. for  $\text{C}_{34}\text{H}_{46}\text{N}_6\text{O}_2$   $[\text{M}+\text{H}]^+ = 571.3682$ , found 571.7406 (figure S1).  $^1\text{H}$  NMR (400MHz,  $\text{CDCl}_3$ ):  $\delta = 7.89(\text{d}, 1\text{H})$ ;  $7.47(\text{m}, 2\text{H})$ ;  $7.12(\text{d}, 1\text{H})$ ;  $6.40(\text{d}, 4\text{H})$ ;  $6.28(\text{d}, 2\text{H})$ ,  $3.35(\text{m}, 8\text{H})$ ;  $3.17(\text{t}, 2\text{H})$ ,  $2.63(\text{t}, 4\text{H})$ ;  $2.41(\text{t}, 4\text{H})$ ,  $2.22(\text{t}, 4\text{H})$ ;  $1.26(\text{s}, 4\text{H})$ ;  $1.18(\text{t}, 12\text{H})$  (figure S2).  $^{13}\text{C}$  NMR (100MHz,  $\text{CDCl}_3$ ): 167.84, 153.53, 152.88, 148.83, 132.45, 128.95, 128.21, 123.86, 122.75, 108.11, 105.50, 97.62, 75.45, 65.05, 55.50, 44.40, 39.12, 29.78, 12.59 (figure S3).



**Scheme S2** Synthetic route for RBTren

### S3. Optimization of experimental condition

Initially the structural and optical stability of the probe RTOC and  $\text{RTOC-Hg}^{2+}$  were investigated within a wide temperature range (20-40°C). However, no such significant change in absorption intensities were observed for both the probes within the aforementioned temperature range (Figure S18 and S19). Therefore, we have decided to perform all the experiments at room temperature i.e., 25°C. To understand the response time of the probe RTOC toward  $\text{Hg}^{2+}$ , a time-dependent absorption spectra of RTOC in the presence of 1 equiv. of  $\text{Hg}^{2+}$  were recorded. The plot of absorption vs. time indicates that the absorption intensity increases up to 15 minutes and then saturated (Figure S13). On the similar lines, ( $\text{RTOC-Hg}^{2+}$ ) system was further interacted with  $\text{S}^{2-}$  and the corresponding absorption vs. time plot shows that the maximum absorption intensity reaches at about 18 minutes (Figure S15). Considering all the parameters, experiments pertaining to RTOC were performed at 25°C with 15 minutes incubation time, whereas the experiments relating to ( $\text{RTOC-Hg}^{2+}$ ) were conducted at 25°C with 18 minutes incubation time.

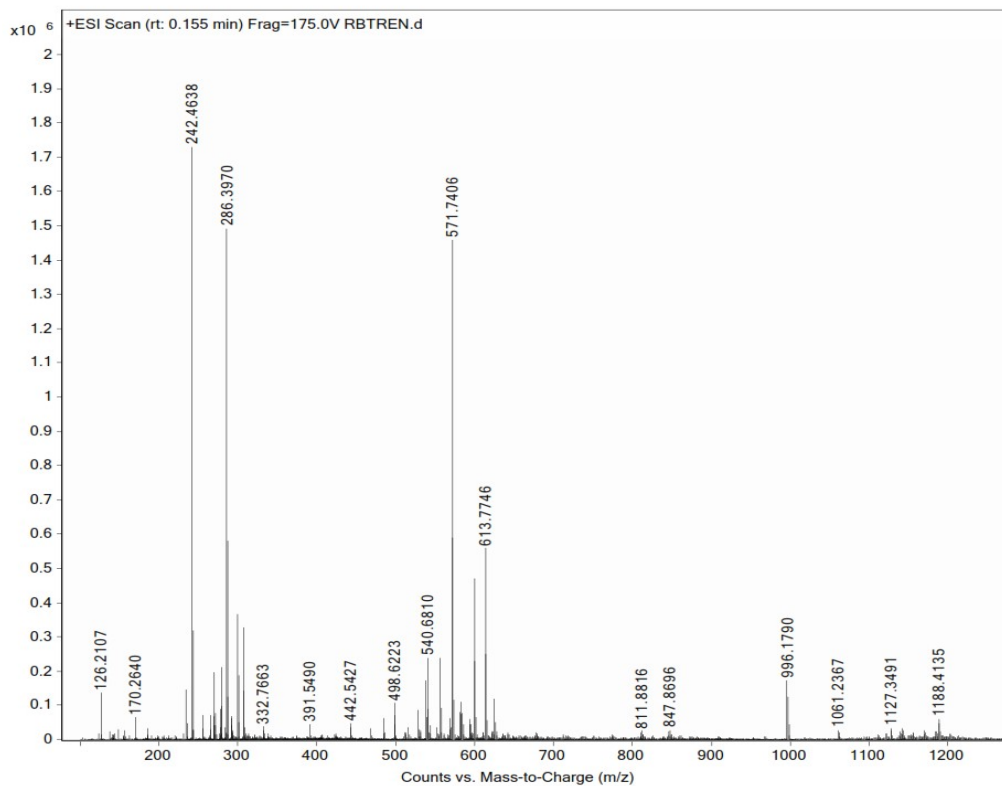


Figure S1 ESI-MS spectrum of RBTren

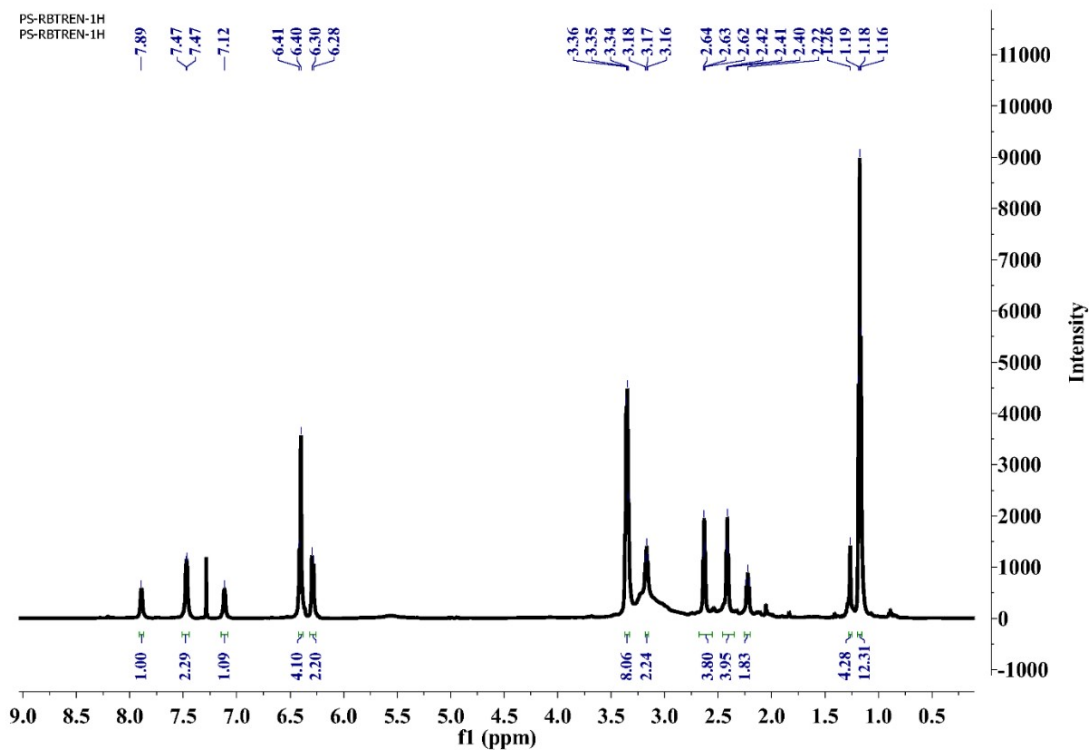


Figure S2 <sup>1</sup>H-NMR spectrum of RBTren in CDCl<sub>3</sub>

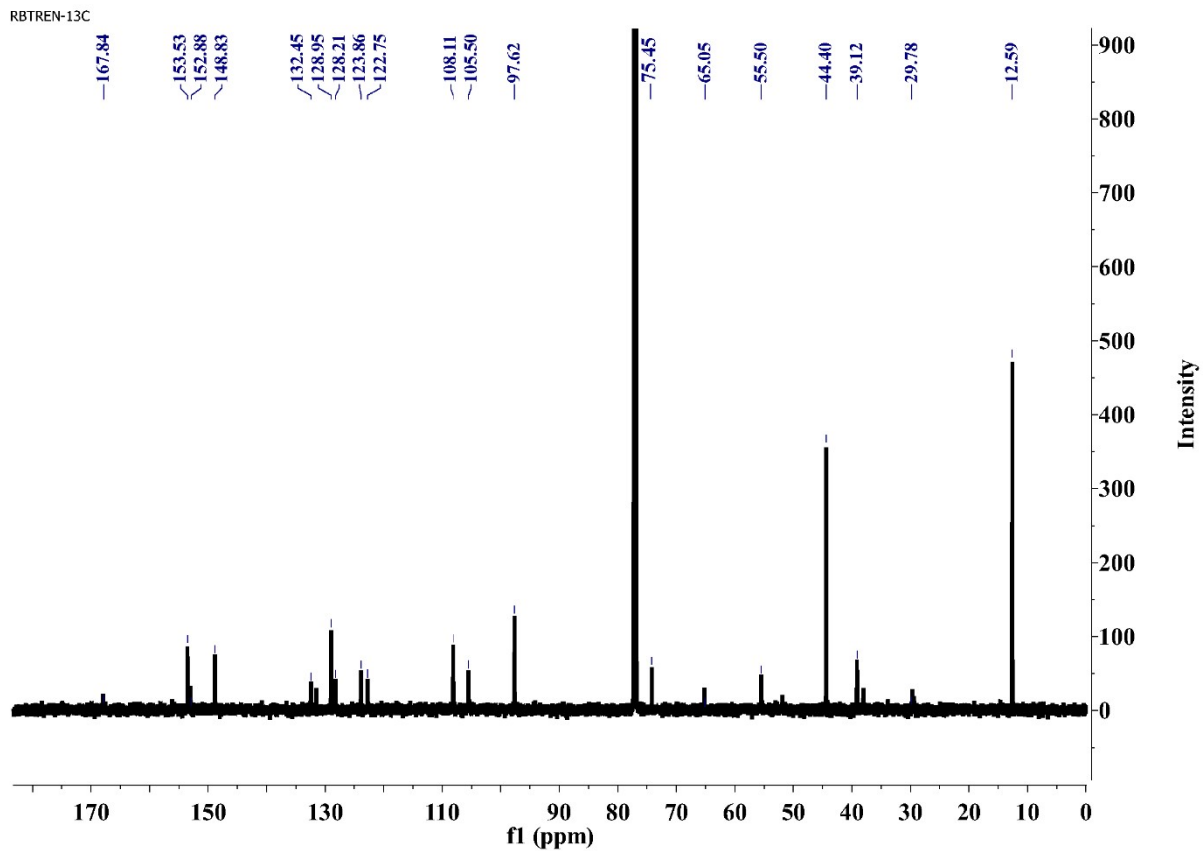


Figure S3  $^{13}\text{C}$  NMR spectrum of RB-Tren in  $\text{CDCl}_3$

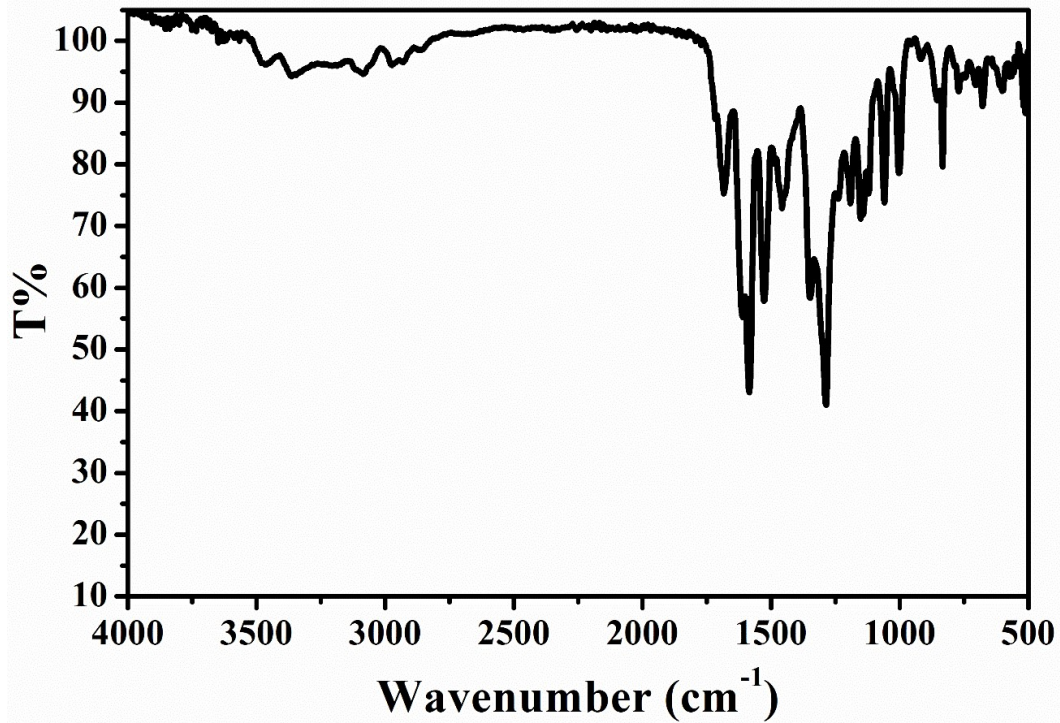


Figure S4 FTIR spectrum of RTOC

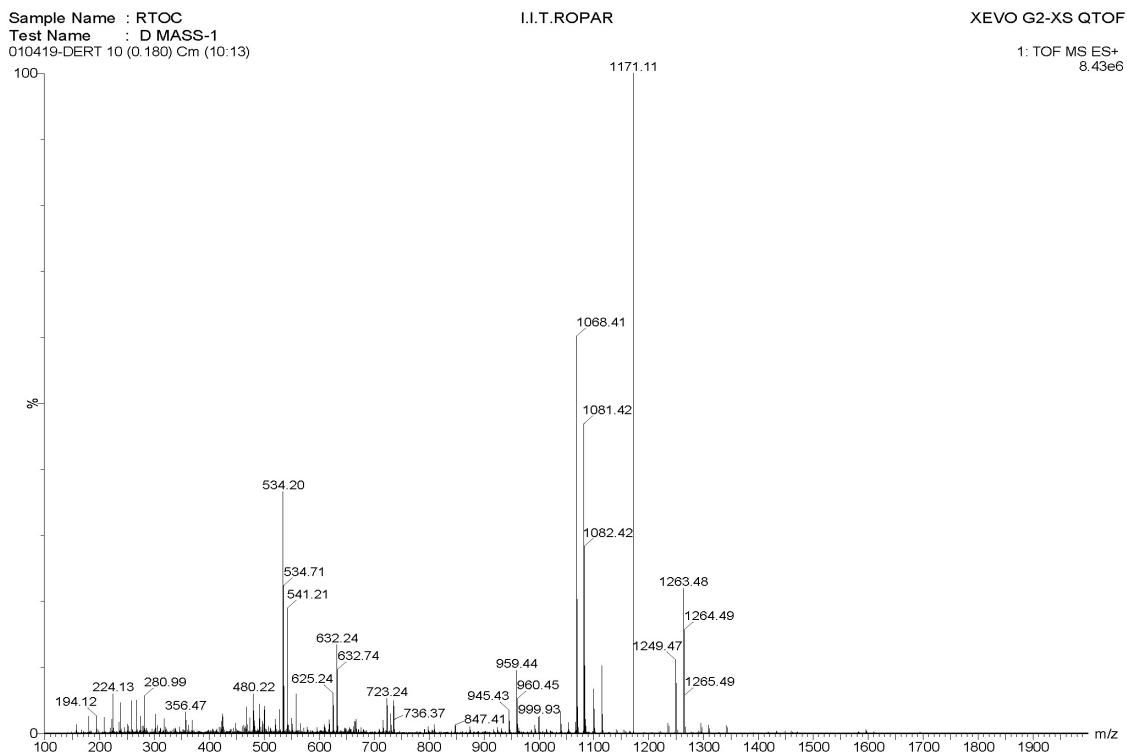


Figure S5 ESI-MS spectra of RTOC

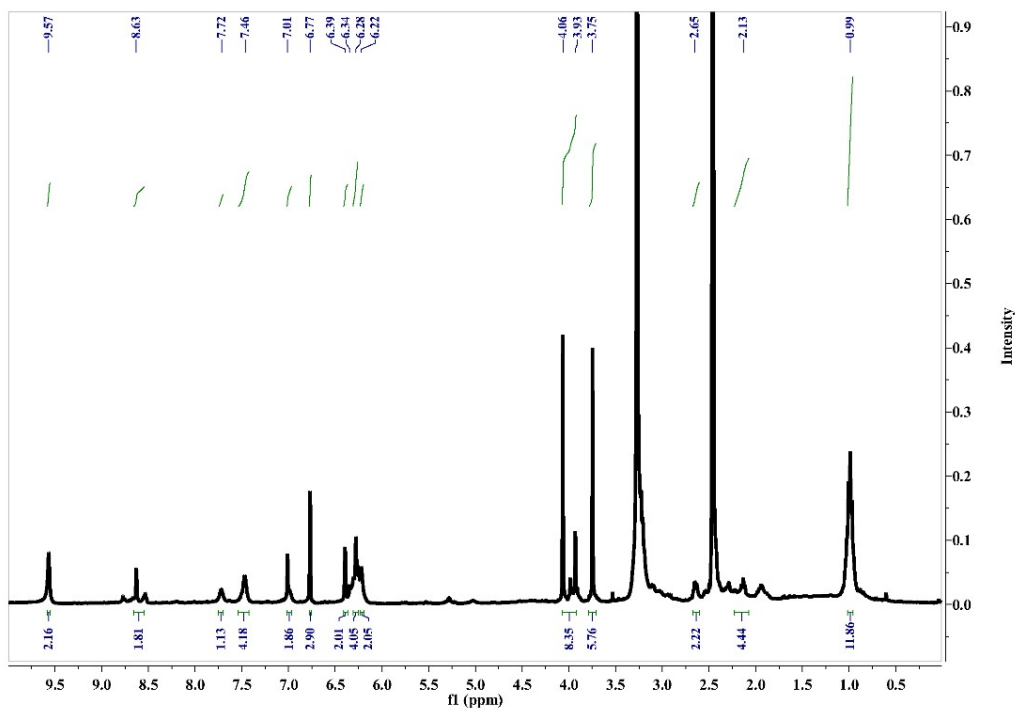


Figure S6  $^1\text{H}$  NMR spectrum of RTOC in  $\text{DMSO-}d_6$

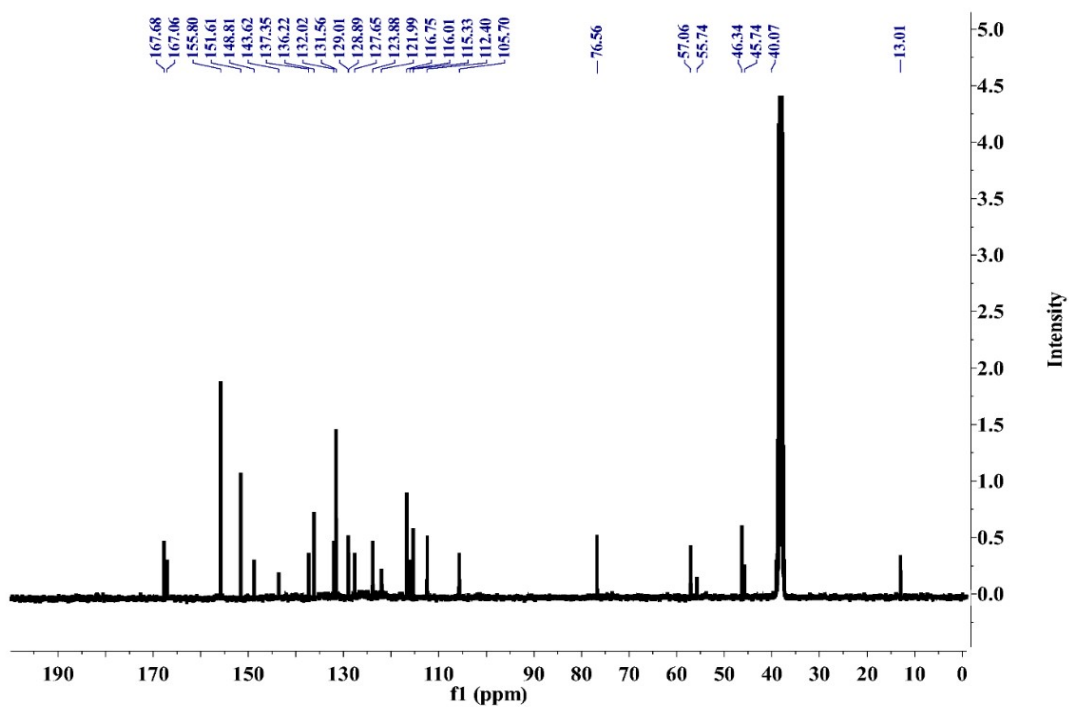
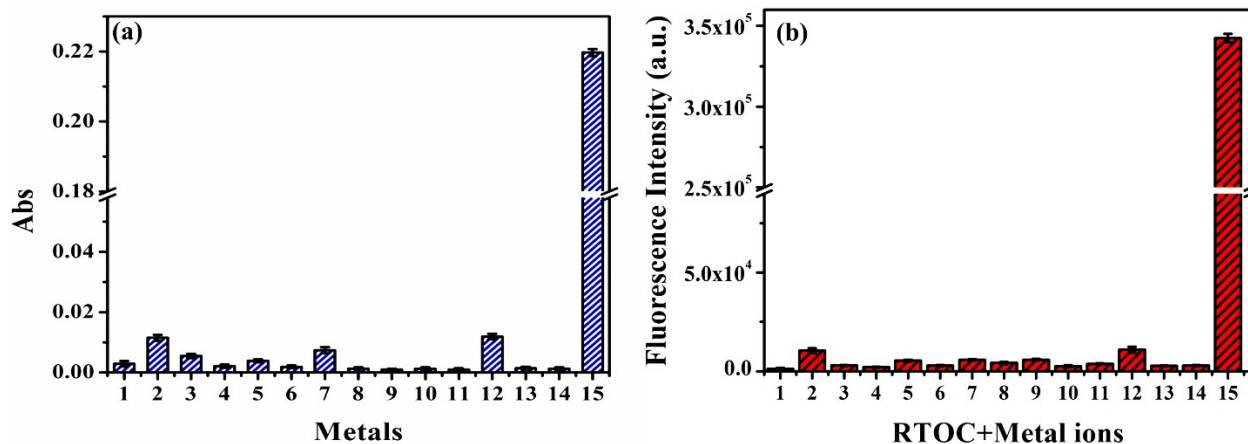
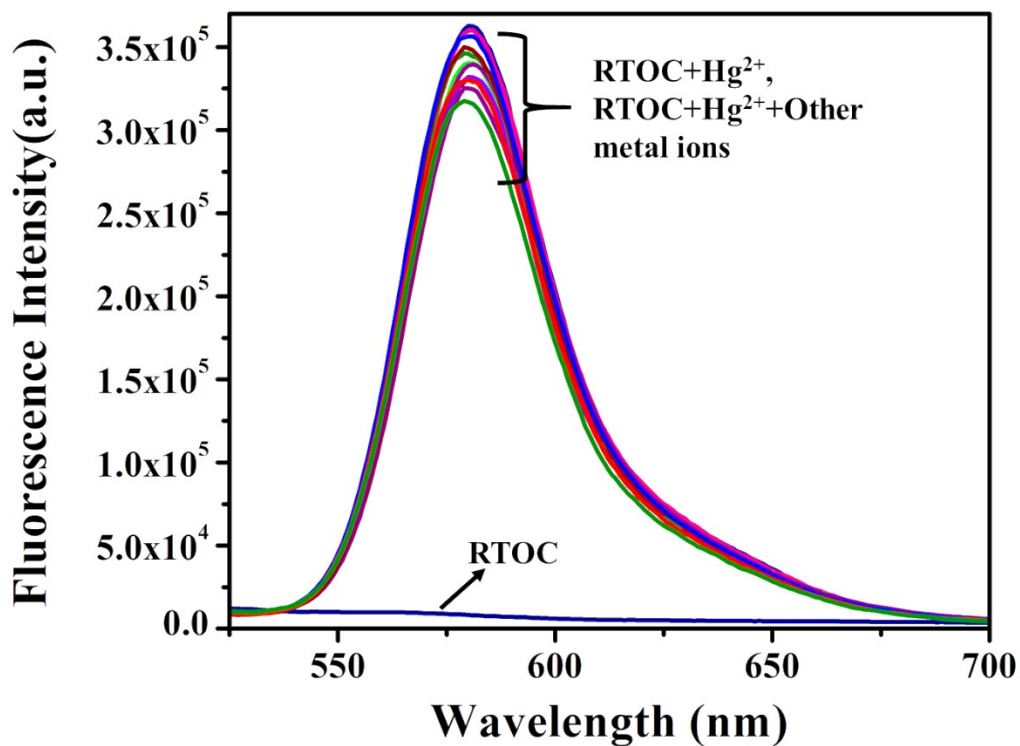


Figure S7  $^{13}\text{C}$  NMR spectrum of RTOC in  $\text{DMSO-}d_6$



**Figure S8** Bar diagram representing the change in (a) absorption and (b) emission spectra of RTOC ( $1.0 \times 10^{-5}$  M) upon addition of different metal ions (1  $\rightarrow$  RTOC, 2  $\rightarrow$  Fe<sup>2+</sup>, 3  $\rightarrow$  Fe<sup>3+</sup>, 4  $\rightarrow$  Cu<sup>2+</sup>, 5  $\rightarrow$  Ni<sup>2+</sup>, 6  $\rightarrow$  Cd<sup>2+</sup>, 7  $\rightarrow$  Co<sup>2+</sup>, 8  $\rightarrow$  Zn<sup>2+</sup>, 9  $\rightarrow$  Sr<sup>2+</sup>, 10  $\rightarrow$  Mn<sup>2+</sup>, 11  $\rightarrow$  Mg<sup>2+</sup>, 12  $\rightarrow$  Pb<sup>2+</sup>, 13  $\rightarrow$  Al<sup>3+</sup>, 14  $\rightarrow$  Cr<sup>3+</sup> and 15  $\rightarrow$  Hg<sup>2+</sup>) in acetonitrile



**Figure S9** Competitive emission spectra of RTOC-Hg<sup>2+</sup> complex in the presence of other metal ions (10 equiv.) in acetonitrile solution

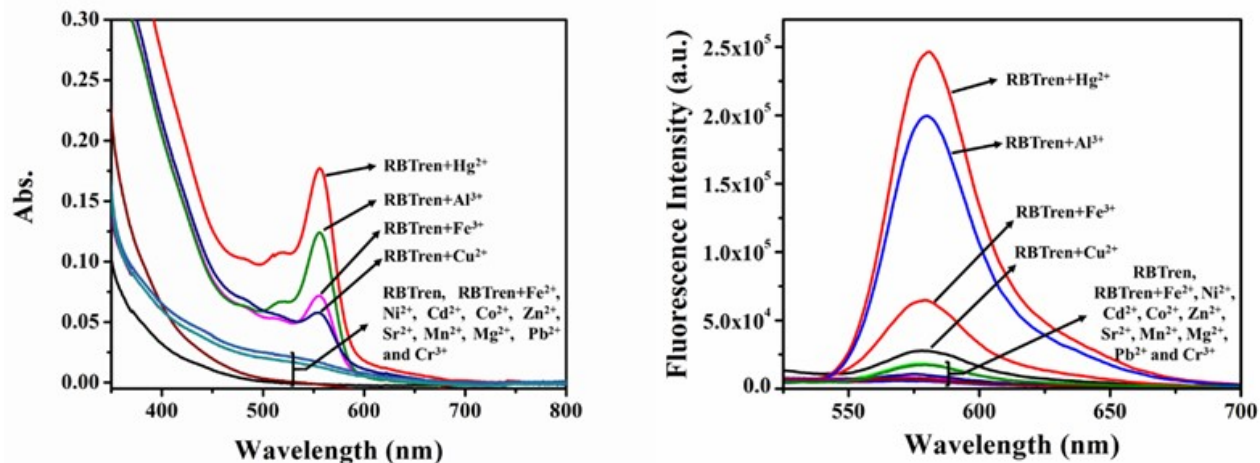


**Figure S10** (a) Absorption spectra of RBTren ( $1.0 \times 10^{-5} \text{M}$ ) with 1 equiv. of different metal ions (b) Emission spectra of RBTren ( $1.0 \times 10^{-5} \text{M}$ ) with 1equiv. of different metal ions

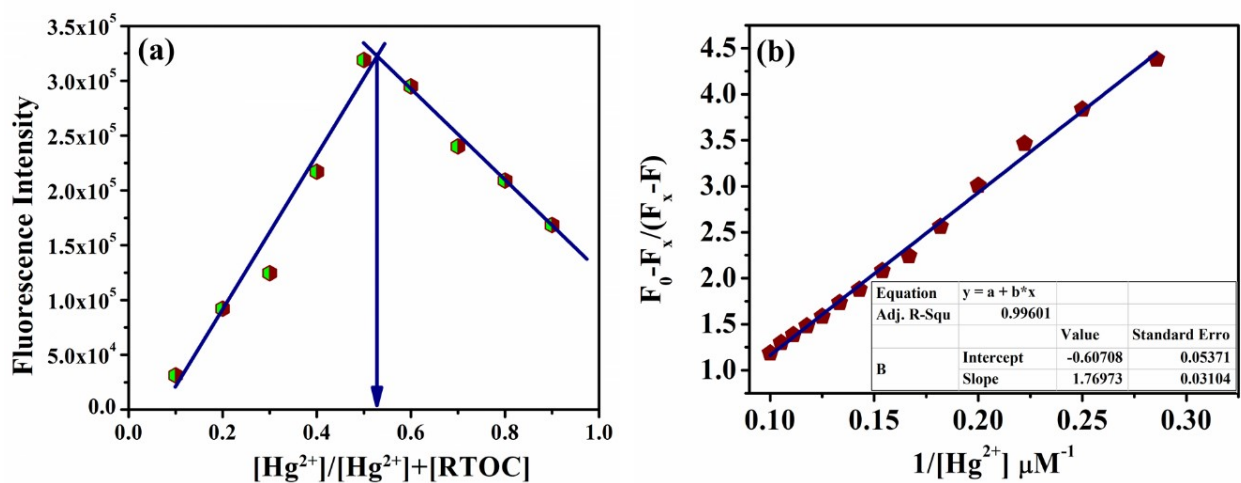


**Figure S11** (a) Jobs plot for receptor RTOC ( $1.0 \times 10^{-5} \text{M}$ ) with  $\text{Hg}^{2+}$  at 582nm (b) Benesi-Hildebrand plot for linear binding constant curve for receptor RTOC ( $1.0 \times 10^{-5} \text{M}$ ) and  $\text{Hg}^{2+}$  (0-30 $\mu\text{M}$ ) complexation



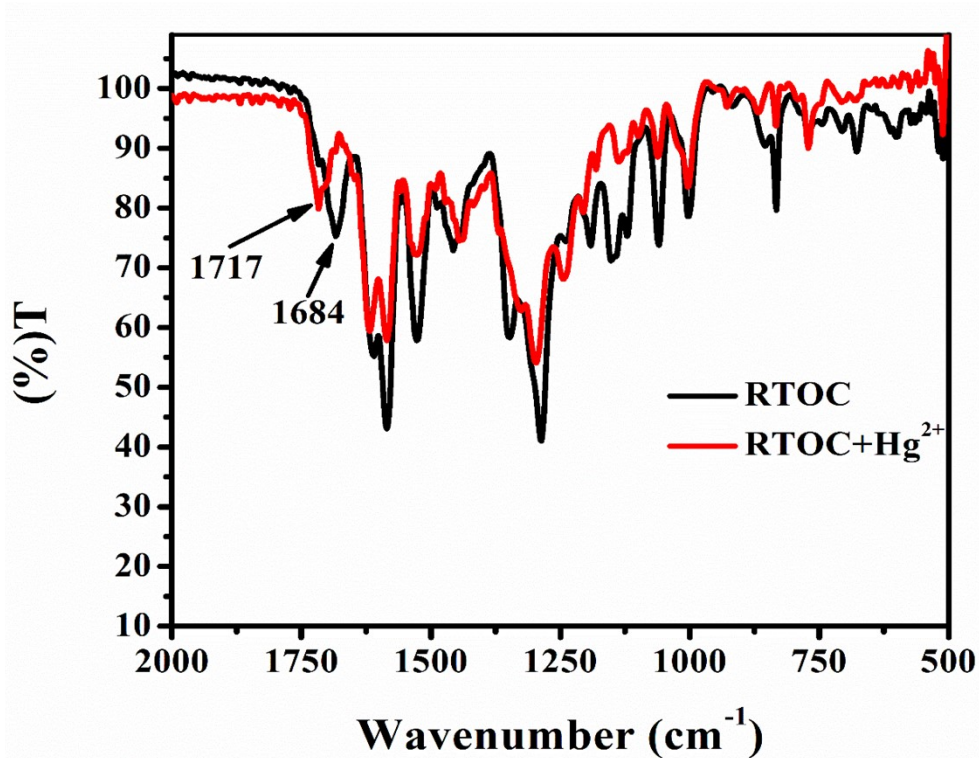


Figure S12 FTIR spectral study of RTOC (black curve) and RTOC-Hg<sup>2+</sup> (red curve) complex after 15mins

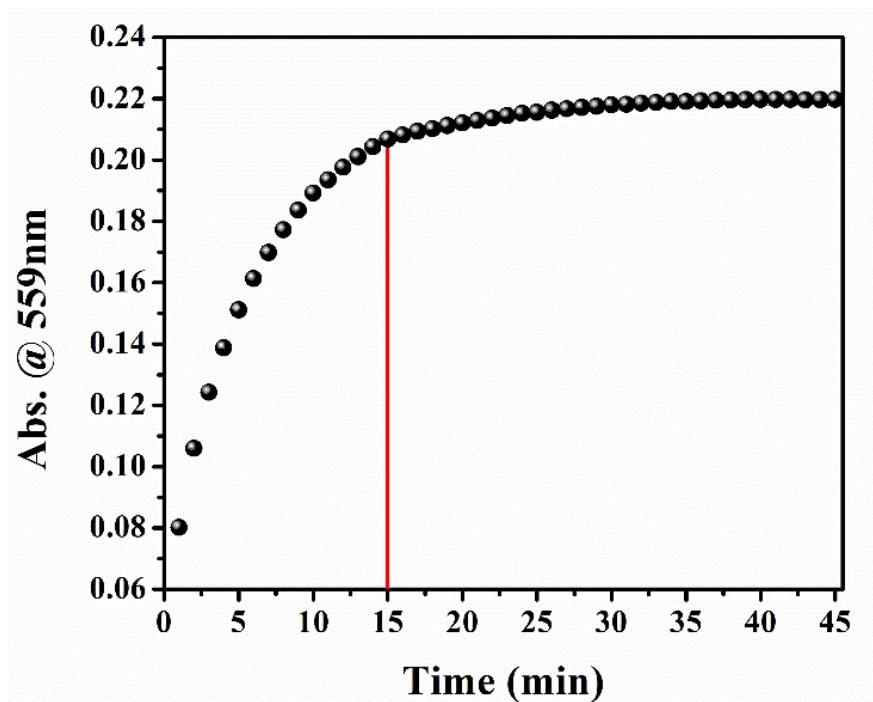
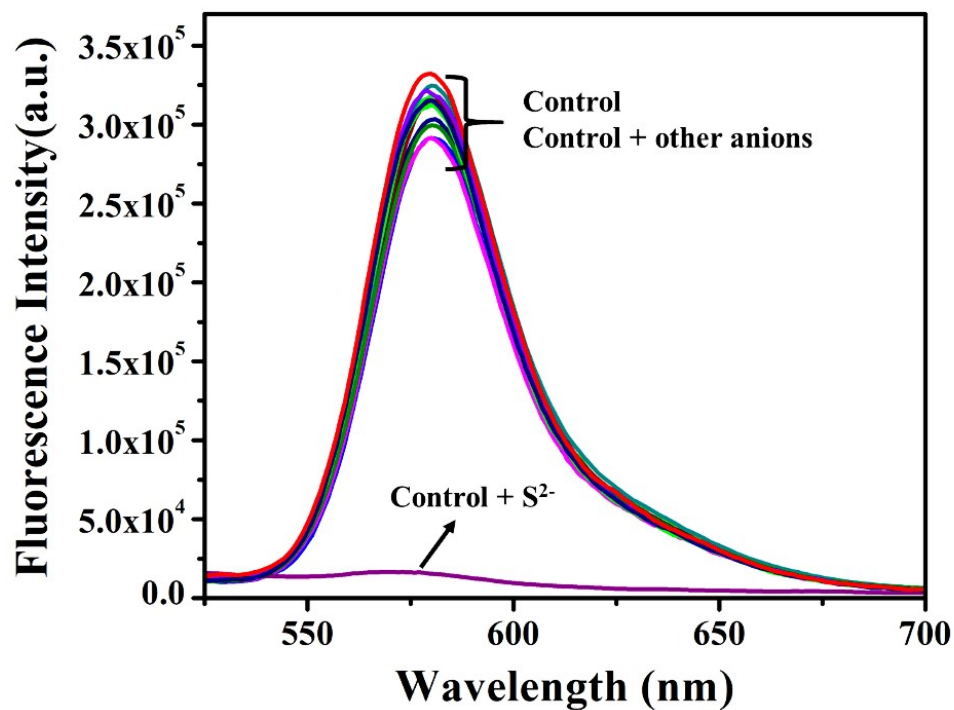
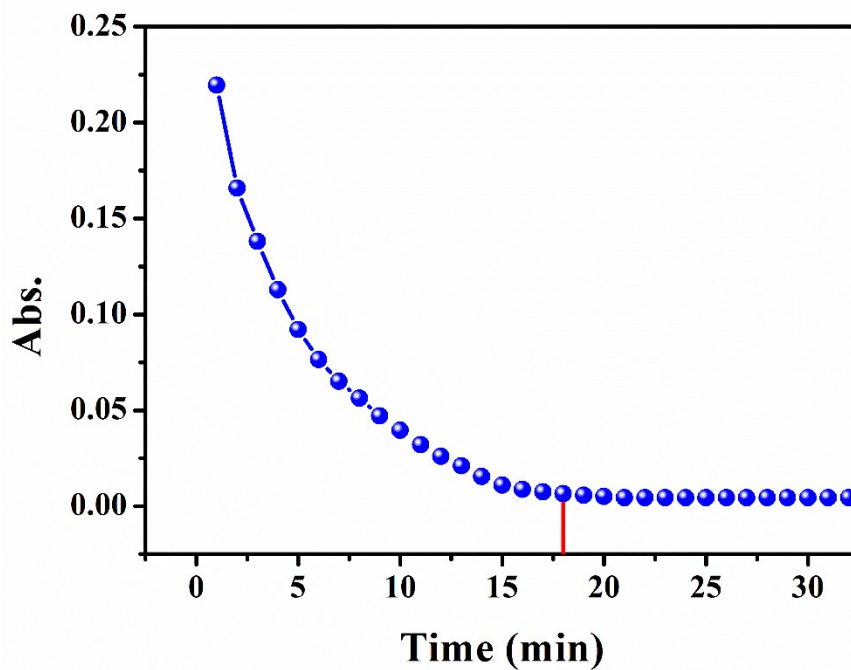


Figure S13 Change in absorption of RTOC ( $\lambda_{\text{max}} = 559\text{nm}$ ) with time after mixing with 10equiv. amount of Hg<sup>2+</sup> ions in acetonitrile



**Figure S14** Relative change in emission intensity upon addition of various anions to the solution of RTOC+Hg<sup>2+</sup> complex ( $1.0 \times 10^{-5}$  M) in acetonitrile ( $\lambda_{\text{ex}} = 510\text{nm}$ )



**Figure S15** Change in absorption of RTOC+Hg<sup>2+</sup> ( $\lambda_{\text{max}} = 559\text{nm}$ ) with time after mixing with 10equiv. amount of S<sup>2-</sup> ions in acetonitrile

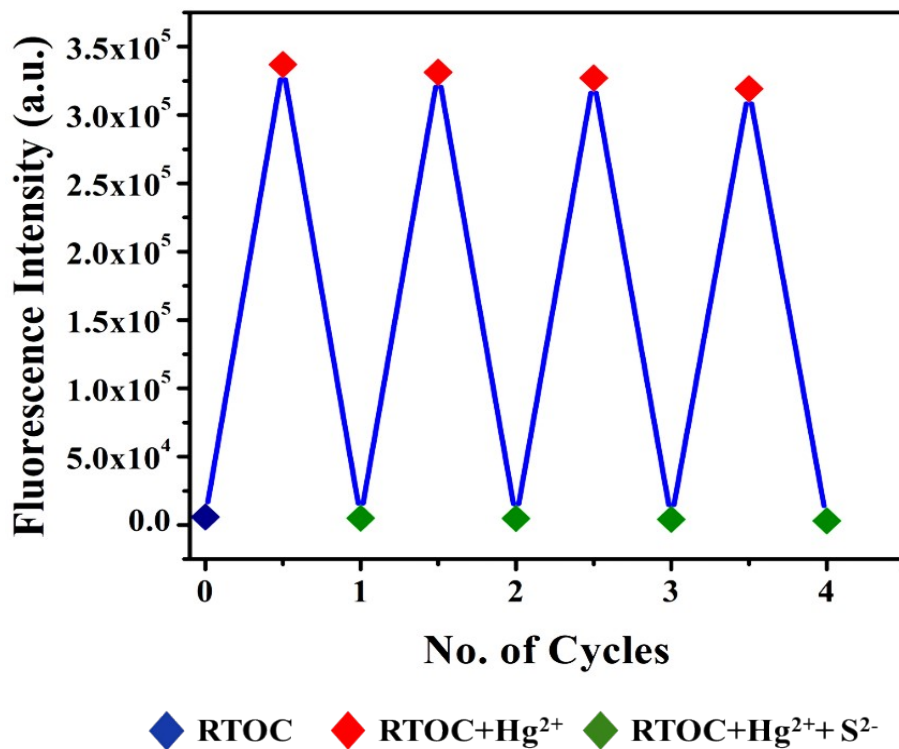


Figure S16 Recyclability of Hg<sup>2+</sup> coordination to RTOC by S<sup>2-</sup>

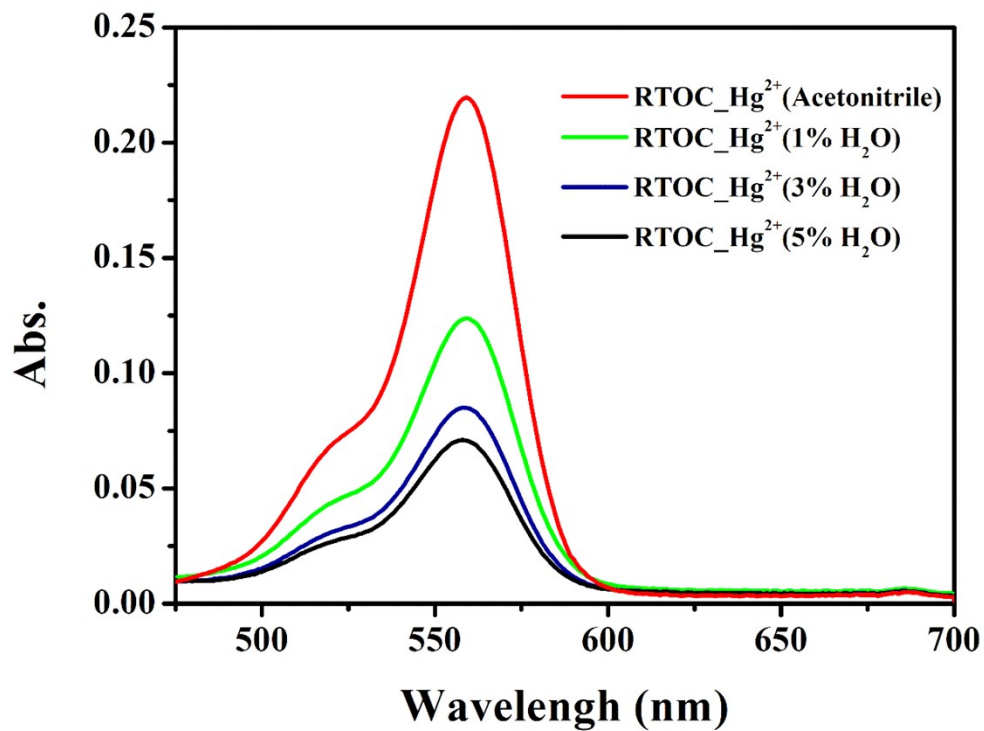


Figure S17 Change in absorption intensities of RTOC+Hg<sup>2+</sup> (1.0x10<sup>-5</sup>M) system upon incremental addition of water

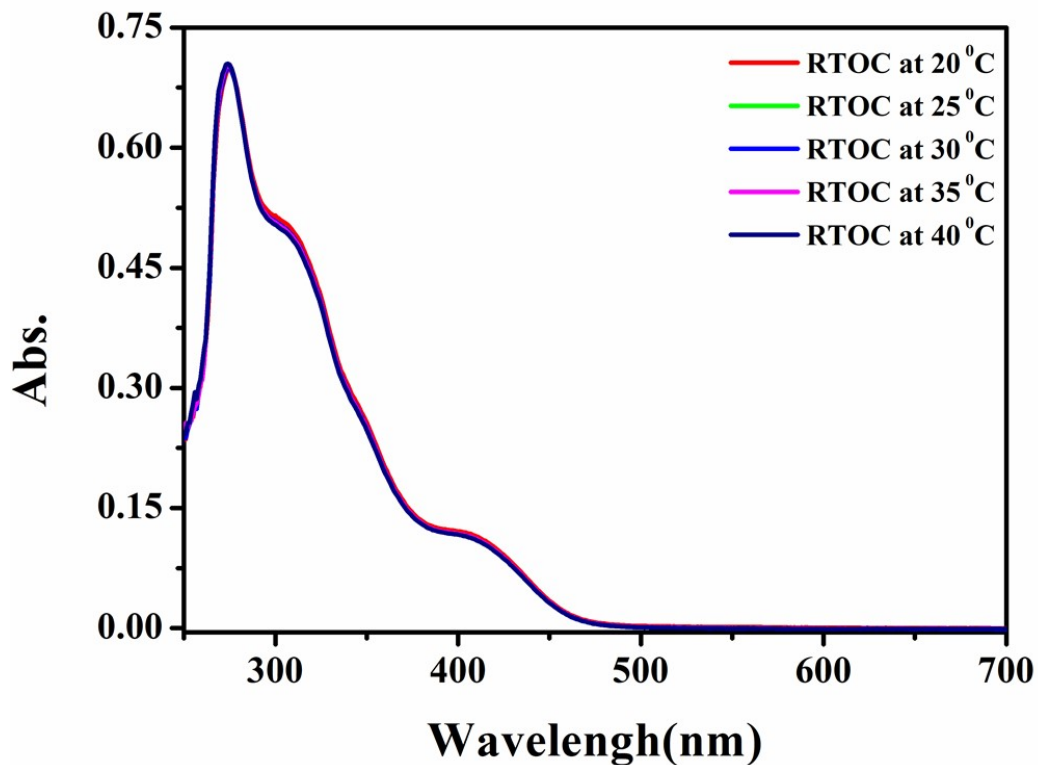


Figure S18 Temperature dependent UV spectra of RTOC ( $1.0 \times 10^{-5} \text{M}$ ) in acetonitrile solution

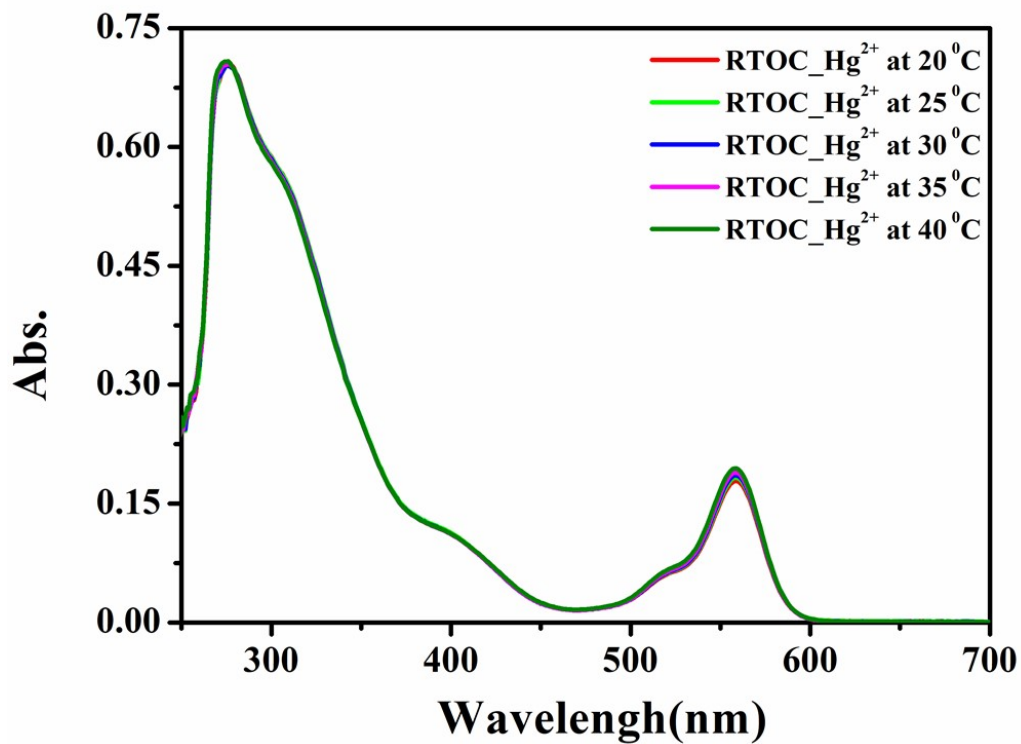


Figure S19 Temperature dependent UV spectra of RTOC ( $1.0 \times 10^{-5} \text{M}$ ) in presence of  $\text{Hg}^{2+}$  in acetonitrile solution